

Chapter 1

Recent Results from the ANTARES Neutrino Telescope

Paschal Coyle

*Centre de Physique des Particules de Marseille,
163 Avenue de Luminy, Case 902, Marseille 13288 cedex 09, France
coyle@cppm.in2p3.fr*

Clancy W. James

*Friedrich-Alexander-Universität Erlangen-Nürnberg,
Erlangen Centre for Astroparticle Physics,
Erwin-Rommel-Str. 1, 91058 Erlangen, Germany
clancy.james@physik.uni-erlangen.de*

for the ANTARES Collaboration

The ANTARES deep sea neutrino telescope has been taking data continuously since its completion in 2008. With its excellent view of the Galactic plane and good angular resolution the telescope can constrain the origin of the diffuse astrophysical neutrino flux reported by IceCube. Assuming various spectral indices for the energy spectrum of neutrino emitters, the Southern sky and in particular central regions of our Galaxy have been studied searching for point-like objects, for extended regions of emission, and for signal from transient objects selected through multi-messenger observations. For the first time, cascade events are used for these searches.

ANTARES has also provided results on searches for hypothetical particles (such as magnetic monopoles and nuclearites in the cosmic radiation), and multi-messenger studies of the sky in combination with various detectors. Of particular note are the searches for dark matter: the limits obtained for the spin-dependent WIMP-nucleon cross section surpassing those of current direct-detection experiments.

1. Introduction

Being weakly interacting the neutrino is unique and complementary to other astrophysical probes such as multi-wavelength light and charged cosmic rays. The neutrino can escape from regions of dense matter or radiation fields and can travel cosmological distances without being absorbed. Neutrinos make it possible to distinguish unambiguously between hadronic and electronic acceleration and to localise these acceleration sites more precisely than cosmic rays detectors. High-energy neu-

trinos may also be produced by the annihilation of dark matter particles which may have accumulated in the cores of massive astrophysical objects such as the Sun. Since the recent observation of a diffuse flux of cosmic neutrinos by the IceCube Collaboration, an understanding of its origin has become a top priority for the astroparticle physics community.

The ANTARES neutrino telescope being located in the Northern Hemisphere has a good visibility for the Galactic plane and, due to the exceptional optical properties of the deep seawater, provides an excellent angular resolution on the neutrino direction. The ANTARES detector (see Ref. [1] for details), is located 40 km offshore from Toulon at a depth of 2475 m. It was completed on 29 May 2008, making it the largest neutrino telescope in the northern hemisphere and the first to operate in the deep sea. The telescope is optimised to detect upgoing high energy neutrinos (> 10 GeV) by observing the Cherenkov light produced in seawater from secondary charged leptons that originate in neutrino interactions near the vicinity of the instrumented volume. Because of the long range of the muon, neutrino interaction vertices tens of kilometres away from the detector can be observed thereby increasing the effective volume. Other neutrino flavours are also detected, although with lower efficiency and degraded angular precision because of the shorter range of the corresponding leptons.

The detector infrastructure comprises 12 mooring lines hosting light sensors. Due to its location in the deep sea, the infrastructure also provides opportunities for innovative measurements in Earth and sea sciences (see for example Ref. [3]). Another project benefiting from the deep sea infrastructure is an R&D system of hydrophones which investigates the detection of ultra-high energy neutrinos using the sound produced by their interaction in water. This system called AMADEUS (Antares Modules for the Acoustic Detection Under the Sea) [4] is a feasibility study for a prospective future large-scale acoustic detector.

The decommissioning of the ANTARES telescope is planned for 2017, at which point the KM3NeT neutrino telescope [2] will have surpassed ANTARES in sensitivity.

2. General Description of the detector

A schematic view of the ANTARES neutrino telescope is given in Fig. 1. The basic detection element is the Optical Module which houses a 10 inch photo-multiplier tube inside a pressure-resistant glass sphere. Each node of the three-dimensional telescope array is the assembly of a mechanical structure, which supports three optical modules, looking downwards at 45° , and a titanium container housing the offshore electronics and embedded processors. In its nominal configuration, a detector line comprises 25 storeys linked together with an electro-mechanical cable. The distance between storeys is 14.5 m with the first storey starting 100 m from the seabed. The line is anchored on the seabed and is held vertical by a submerged buoy. The full neutrino telescope comprises 12 lines, 11 with the nominal configuration,

the twelfth line being equipped with 20 storeys and completed by devices dedicated to acoustic detection. Thus, the total number of the OMs installed in the detector is 885. The lines are arranged in an octagonal configuration, with a typical interline spacing of 60-70 m. The infrastructure is completed by the Instrumentation Line, which supports the instruments used to perform environmental measurements.

The detection lines are flexible and variations in the intensity and direction of the sea current can induce a coherent displacement, typically of the order of a few meters for the uppermost storeys. In addition, the storeys may rotate about the vertical axis. For the ultimate precision on the neutrino directions it is important to follow such movements. An acoustic positioning system [5] and compasses within the electronics container provide a few centimetre and few degree precision on the Optical Module position and orientation.

The data communication and the power distribution to the lines are provided via a network of interlink cables and a junction box on the sea floor. Power is transmitted in alternating current from shore, via a single conductor in a 42 km long electro-optic cable, to a transformer in the junction box; the power return is via the sea.

The data acquisition system is based on the ‘all-data-to-shore’ concept. In this mode, all signals from the PMTs that pass a preset threshold (typically 0.3 single photo electrons) are digitised in a custom built ASIC chip and all digital data are sent to shore, via an optical Dense Wavelength Division Multiplexing system. On shore the data are processed in real-time by a farm of commodity PCs. The data

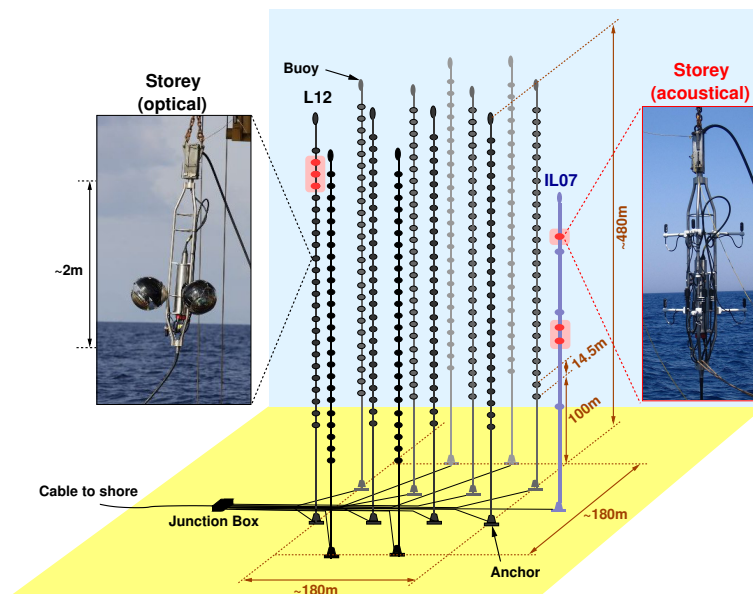


Fig. 1. Schematic view of the ANTARES detector.

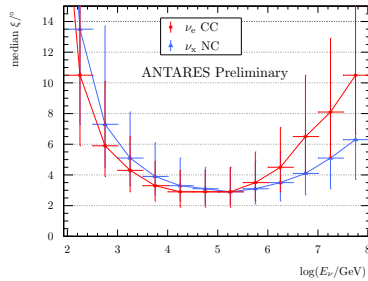


Fig. 2. Angular resolution for cascade topology events.

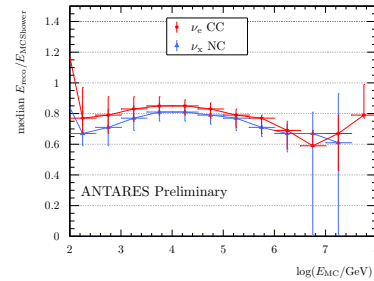


Fig. 3. Energy resolution for cascade topology events.

flow is typically a couple of Gb/s and is dominated by the light generated by K40 decays of the salt in the seawater (typically a 50 kHz baseline singles rate per photo-multiplier).

3. Event Reconstruction

The main channel for the search for astrophysical point-like sources of neutrinos is the muon neutrino. The high rate of downgoing μ from the interactions of cosmic rays in the atmosphere restricts such searches to events coming from below, or only a few degrees above, the horizon. The remaining background is then the flux of atmospheric ν_μ and those few remaining atmospheric μ events misreconstructed as upgoing. The long scattering length of blue light in seawater provides an excellent directional resolution on the ν_μ primary of 0.38° for an E^{-2} source [6]. Thus, angular clustering requirements yield a strong suppression of both backgrounds.

The effective area of neutrino telescopes such as ANTARES and IceCube to cascade events (neutral-current (NC) interactions, and ν_e and ν_τ charged-current (CC) interactions) is generally lower than that of ν_μ CC interactions, due to the shorter range of the outgoing lepton. Additionally, the angular resolution of the cascade channel is inferior. Nevertheless, it has several advantages: neutrino events are more easily distinguished from the background of atmospheric muons, allowing both up- and down-going events to be studied. Furthermore, the energy deposited in the detector is better correlated with the energy of the primary neutrino.

The performance of the current ANTARES cascade reconstruction algorithm [7] yields a median angular resolution of typically 3° for the energy range 10-100 TeV (Fig. 2). The corresponding energy resolution is about 5% (Fig. 3) and thus is limited by the current systematic uncertainty of 10%. Below 10 TeV, the resolution degrades due the reduced number of detected photons, while above 300 TeV the events start to saturate the detector.

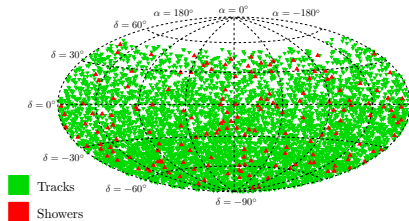


Fig. 4. Arrival directions of events in the all-sky point source analysis.

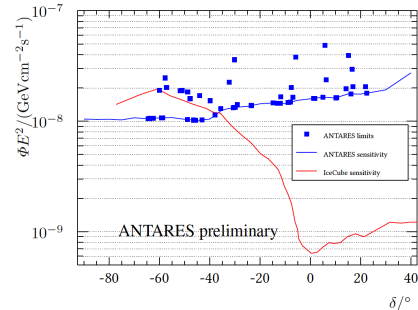


Fig. 5. Limits and sensitivity of the ANTARES targeted source for flavour uniform neutrino point sources with an E^{-2} spectra in terms of flux per flavour.

4. Point source searches for astrophysical neutrinos

The inclusion of the cascade channel has allowed for the first time a combined point-source search using both muon-track and cascade events using 1690 days of effective livetime from 2007 to 2013 [7]. After cuts, the sample consisted of 6261 muon-track events, and 156 cascade events, with an estimated contamination of 10% mis-reconstructed atmospheric muons in each. The resulting skymap is shown in Fig. 4.

While the atmospheric background produces predominantly muon-track events, an E^{-2} point source with a flavour-uniform flux would be expected to produce a cascade-to-track ratio of 3:10, significantly increasing the sensitivity of the search. The achieved search sensitivity was approximately $10^{-8} \text{GeV}^{-1} \text{cm}^{-2} \text{s}^{-1}$ for $\delta < -40^\circ$ as shown in Fig. 5. An untargeted point-source search, a search over a list of pre-specified candidates, and a search using the origins of the IceCube events reported in Ref. [8] were applied to this data. No significant excess was observed.

4.1. Joint ANTARES/IceCube Point source search

A joint analysis using ANTARES and IceCube data is detailed in Ref. [9]. The fractional number of source events expected to be present in each data set is shown in Fig. 6 for the current best-fit to the IceCube flux. The results of the combined search are shown in Fig. 7, for an $E^{-2.5}$ source spectrum. The ANTARES contribution is dominant for declination $< -15^\circ$. No significant cluster is found, with the most significant source on the candidate list being the blazar 3C 279, with a pre-trial p-value of 5%. The combined analysis improves on the results from both experiments, indicating the complementarity of the two instruments.

6

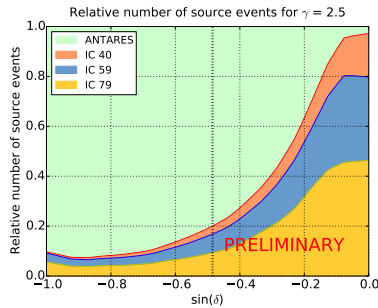


Fig. 6. Fractional contribution of each data set to the total number of signal events passing cuts in the joint ANTARES-IceCube analysis for an $E^{-2.5}$ spectra with no cutoff as a function of δ .

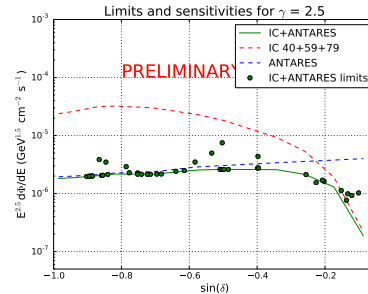


Fig. 7. Sensitivity (lines) and limits (dots) of the joint ANTARES-IceCube analysis for an $E^{-2.5}$ spectra with no cutoff as a function of δ . ANTARES (blue), IceCube (red), combined (green).

4.2. Limits on a point source origin of the IceCube signal

It has been proposed [10] that the cluster of IceCube events seen in Ref. [8] could be due to a single point-like source, which is not detectable due to the poor angular resolution. The non-detection of an ANTARES point-like source in this region, as reported by Ref. [11], limits the flux of such a source as a function of spectral index, shown by the solid lines and y-axis of Fig. 8. The flux required to produce a given number of events in the HESE analysis (x-axis) is also shown. The range where the latter is greater than the former rules out a corresponding contribution from any single point-like source with that spectral index at 90% C.L.. The result above is particularly relevant because the current best-fit spectrum (between 25 TeV and 2.8 PeV) of the IceCube flux has a spectral index of -2.5 ± 0.09 [12]. ANTARES can thus rule out any single point-source of neutrinos in the region of the Galactic Centre with spectral index of -2.5 as having a flux corresponding to more than 2

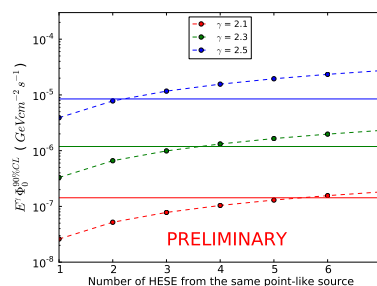


Fig. 8. ANTARES limits (solid lines) at 90% C.L. on the contribution of point-like sources to the IceCube HESE sample for various spectral indices, shown for $\delta = -29^\circ$. These are compared with the flux required to produce a given number of HESE events. Similar results are obtained for other declinations around the Galactic Centre.

HESE events.

5. Transient sources

5.1. Flares from AGN and X-ray binaries

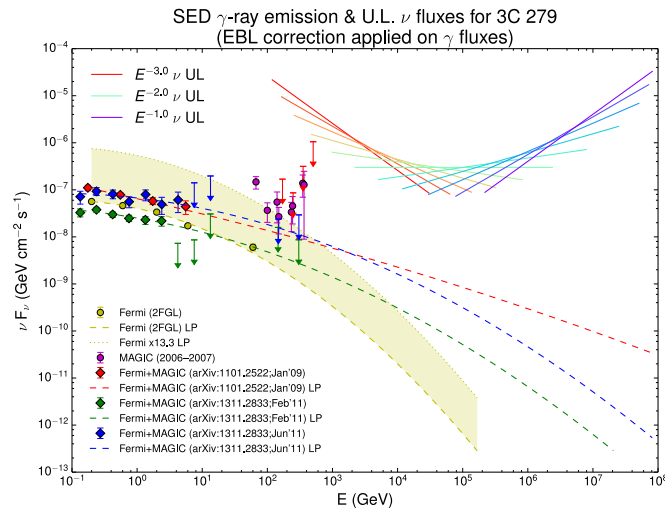


Fig. 9. Limits on the neutrino flux from the blazar 3C279 as a function of spectral index (solid lines), compared to the observed (points) and extrapolated (dashed lines) gamma-ray spectra observed by FERMI and IACTs.

Active galactic nuclei (AGN) have long been proposed as a source of high-energy cosmic rays and, hence, neutrinos [13]. Blazars, AGNs with jets pointing towards the line-of-sight, exhibit bright flares which dominate the extragalactic gamma-ray sky observed by Fermi-LAT [14].

Using multi-wavelength observations, several bright blazars have been reported by the TANAMI Collaboration [15] to lie within the 50% error bounds of the reconstructed arrival directions of the PeV-scale events IC 14 and IC 20 observed by IceCube. ANTARES observes signal-like events from the two brightest blazars, both in the field of IC 20 [16], although this is also consistent with background fluctuations. A lack of such events from the field of IC 14 excludes a neutrino spectrum softer than $E^{-2.4}$ as being responsible for this event. The highest-energy event IC 35 (“Big Bird”) was detected during an extremely bright flare from the blazar PKS B1424-418, which lies within the 50% error region of the IC 35 arrival direction. ANTARES finds only one event within 5° of this source during the flaring period, whereas approximately three would be expected from random background fluctuations alone.

In another analysis [17], ANTARES targets a sample of 41 blazar flares observed

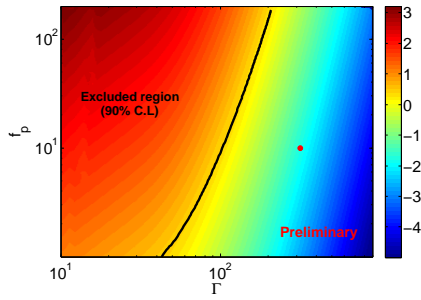


Fig. 10. Range of jet Γ -factor and baryonic loading f_p excluded by ANTARES in the case of GRB110918A using the NeuCosmA model of Ref. [20], as described in Ref. [21]. The assumed values of $\Gamma = 316$ and $f_p = 10$ are shown by the red point, while the colour-coding gives the expected number of observable neutrinos.

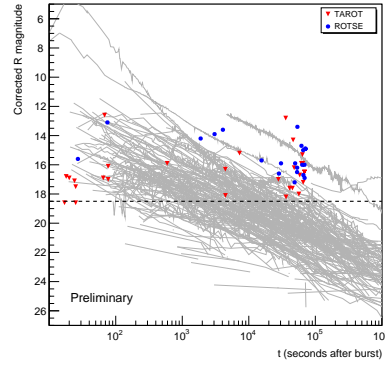


Fig. 11. Limiting magnitudes and delay times of optical follow-up observations to ANTARES alerts with ROTSE and TAROT [22] compared to (grey lines) the light-curves from measured GRBs.

by Fermi LAT and 7 by the IACTs H.E.S.S., MAGIC, and VERITAS. The lowest pre-trial p-value of 3.3% was found for the blazar 3C 279, which comes from the coincidence of one event with a 2008 flare previously reported in Ref. [18]. However, the post-trial p-value is not significant. The resulting limits are given in Fig. 9.

Similar methods were also used to search for neutrino emission during the flares from galactic x-ray binaries [19]. A total of 34 x-ray- and gamma-ray-selected binaries were studied, with no significant detections, allowing some of the more optimistic models for hadronic acceleration in these sources to be rejected at 90% C.L..

5.2. Gamma ray bursts

Long-duration gamma-ray bursts (GRBs) have been proposed as a source of the highest-energy cosmic rays [23]. ANTARES has searched for a neutrino flux from GRBs considering two models of the emission processes: the NeuCosmA description of Ref. [20] and the “photospheric” model of Ref. [24]. In each case, the expected signal is simulated on a burst-by-burst basis, and the detector response and background are modelled using the exact detector conditions at the time of the burst. The ANTARES analysis using the NeuCosmA model was developed and applied to a sample of 296 bursts in Ref. [25], with no coincident neutrino events detected. Since then, one especially powerful burst GRB110918A, and the nearby burst GRB130427A, have been identified as promising candidates for neutrino detection, and studied in detail in Ref. [21]. No coincident events are observed from

either burst. The predicted ν emission scales with Γ^{-5} and linearly with f_p , allowing limits to be set on the bulk gamma-factor and baryonic loading of the jet, as shown in Fig. 10.

A search using the photospheric models is developed in Ref. [26], and will shortly be unblinded. The GRB search methods are also being extended to test Lorentz invariance violation [21], which would delay the arrival times of TeV neutrinos compared to GeV photons.

5.3. Optical and X-ray follow-up

The TAToO (telescopes-ANTARES target-of-opportunity) program [27] performs near-real-time reconstruction of muon-track events. If a sufficiently high energy event is reconstructed as coming from below the horizon (i.e. those events most likely to be of astrophysical origin), an alert message is generated to trigger robotic optical telescopes, and, with a higher threshold, the Swift-XRT. The very short alert-generation time (a few seconds) and half-sky simultaneous coverage of ANTARES makes it ideal for detecting transient signals, and optical and x-ray follow up observations have been initiated within 20 s and one hour respectively.

Results from 42 optical and 7 x-ray alerts have been analysed. While no associated transient event was detected, this non-observation can be used to place limits on the astrophysical origin of the detected neutrinos [22], as shown in Fig. 11. The steep fall-off of the light-curves emphasises the need for a rapid alert generation and follow-up: observations within one minute can rule out a GRB origin with high confidence, while those after one day would be unlikely to detect even a bright GRB.

6. Diffuse flux searches

A diffuse flux search in ANTARES has been developed that makes optimal uses of both muon track and cascade events [28]. Since any explicit selection of muon-like and cascade-like events inevitably discards events with topologies falling between the two classes, no such selection was made. The procedure was applied to 913 days of effective livetime between 2007 and 2013. The expected number of events from the standard and prompt atmospheric background [30, 31] was 9.5 ± 2.5 , composed of 5.5 ν_μ CC, 1 atmospheric μ , and 2.9 ν NC and ν_e events. The expectation from the IceCube neutrino flux reported by [8] was 5.0 ± 1.1 events. After unblinding, 12 events passed the selection cuts—consistent with both background only, and background and IceCube diffuse flux expectations. The resulting limits on an E^{-2} flux are given in Fig. 12.

7. Extended source searches

In addition to the numerous point-like candidate neutrino sources, several extended regions have been proposed as hadronic acceleration sites. ANTARES searches

for an excess neutrino flux from these regions using “on-zones” defined by specific templates, which are compared to “off-zones” of exactly the same size and shape, but offset in right ascension. Thus the off-source regions give an unbiased estimate of the background in the source region in a way that is independent of simulations. Results for the Fermi Bubbles, Galactic plane, and the IceCube cluster are described below.

7.1. Fermi bubbles

The Fermi Bubbles [35] are large regions of γ -ray emission extending perpendicular to the Galactic Centre and have been proposed as sites of hadronic acceleration [34], with neutrinos expected from p-p collisions. A first search in ANTARES data from 2008-2011 for emission from these regions was presented in Ref. [33] - here, an update is presented adding 2012-2013 data.

The on- and off-zone regions used in the Fermi Bubble analysis are shown in Fig. 13. Flavour-uniform E^{-2} and $E^{-2.18}$ neutrino fluxes are assumed, where the latter is motivated by the best-fit proton spectrum of $E^{-2.25}$ reported by Ref. [34]. Exponential cut-offs at energies of 500, 100, and 50 TeV are also tested. A slight excess is found in the source region, corresponding to a 1.9σ significance. The corresponding upper limits on an $E^{-2.18}$ neutrino flux are compared in Fig. 14 to the expectations from Ref. [34].

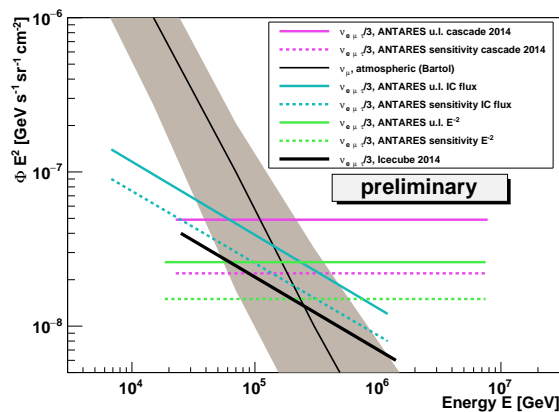


Fig. 12. ANTARES sensitivity to (dotted), and limits on (solid), the diffuse astrophysical neutrino measured by IceCube [28]. Shown are (pink) the previous ANTARES limit on an E^{-2} spectrum [29], and current results on (blue) the flux (thick black line) observed by IceCube [12] and (green) an E^{-2} spectrum. This is compared to the conventional atmospheric background flux (thin black line) [30], with associated error (grey shading).

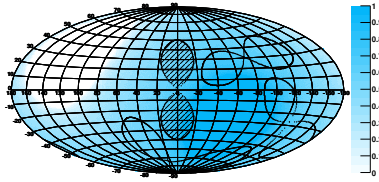


Fig. 13. On- and off-zone search regions for the Fermi Bubble search of Ref. [32], compared to the ANTARES visibility (blue shading).

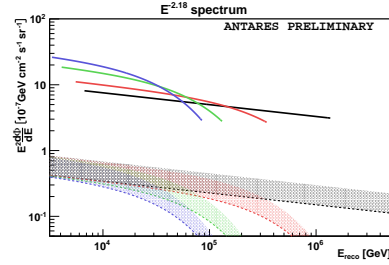


Fig. 14. 90% C.L. upper limits (lines) on the neutrino flux from the Fermi Bubbles, compared to (shaded regions) expectations [34] for different spectral shapes.

7.2. Galactic plane

Cosmic rays in our galaxy will collide with the interstellar medium to produce pions and, hence, neutrinos. Direct evidence for these processes comes from observations by Fermi-LAT [39] of the diffuse galactic gamma-ray background. It is also interesting that the number of IceCube high energy starting events (HESE) in the $E > 100$ TeV range with angular directions consistent with this region corresponds to a flux consistent with that observed in γ -rays [36], as shown in Fig. 15. The large uncertainty in the arrival directions of cascade-like HESE, and their low number, makes this comparison difficult however.

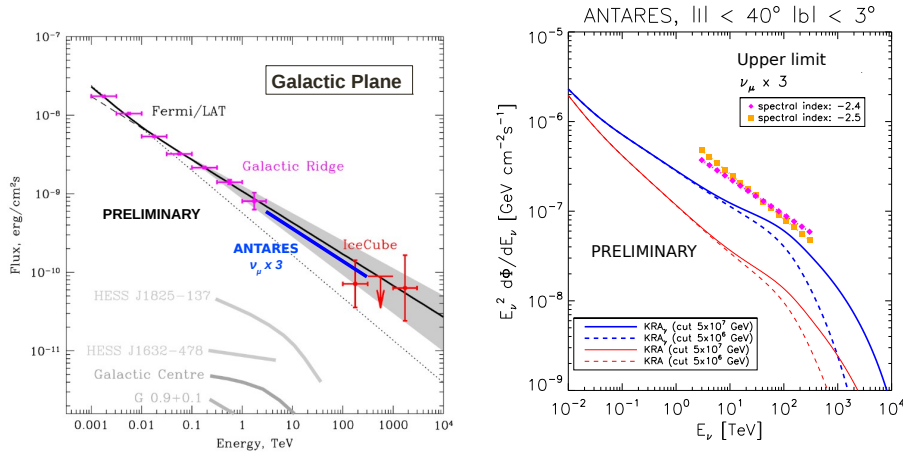


Fig. 15. ANTARES 90% C.L. upper limits for the search for an excess of events from the central Galactic region [37]. Left: for an $E^{-2.4}$ neutrino spectra, compared to the expected neutrino flux (solid black line) extrapolated from the FERMI-LAT diffuse gamma-ray up to high energies. Right: for $E^{-2.4}$ and $E^{-2.5}$ neutrino spectra, compared to the predicted neutrino fluxes from Ref. [38].

The ANTARES northern latitude is ideally suited for studying the expected neutrino flux from the inner galactic plane. A search has been performed in the regions of galactic longitude $|l| < 40^\circ$ and latitude $|b| < 3^\circ$, as reported in [37]. The search used nine off-zones and one on-zone, and found no excess in the on-zone region (one event compared to an average of 2.5 for the off-zones). The resulting limits are shown in Fig. 15. In particular, the hypothesis of a 1 – 1 relation between the γ -ray and neutrino flux from the Galactic Ridge is ruled out at 90% confidence, indicating that ANTARES is already testing the well-established multimessenger γ - ν -CR paradigm in our galaxy. The limits cannot rule out however models from more-detailed simulations of galactic cosmic-ray propagation.

7.3. IceCube cluster

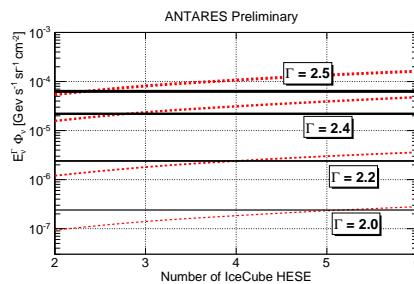


Fig. 16. ANTARES upper limits at 90% C.L. (black) on a flavour-uniform neutrino flux from the IceCube cluster region as a function of the spectral index Γ , compared to (red) the flux required to produce an expected number of events in the IceCube HESE analysis [40]. The maximum number of IceCube events allowed at 90% C.L. is indicated by the crossing points of the red and black lines for a given spectral index. See Ref. [37] for details.

The same techniques employed in the galactic plane search were used to probe the origin of the cluster of IceCube events reported in Ref. [8]. The analysis of Ref. [37] used twelve off-zones and one on-zone to search for an excess of events. One event passing the selection cuts is observed in both the on-zone and the average off-zone, i.e. no excess is observed. Resulting limits on the maximum number of HESE events produced by a source with different spectral indices are presented in Fig. 16. For the best-fit IceCube diffuse spectral index $\Gamma = 2.5$ [12], ANTARES rejects at 90% confidence a flux from this region expected to produce three or more of the IceCube events in the cluster. This extends the results of Refs. [6, 11] for this region, which limit the existence of point- like and mildly extended sources in this region.

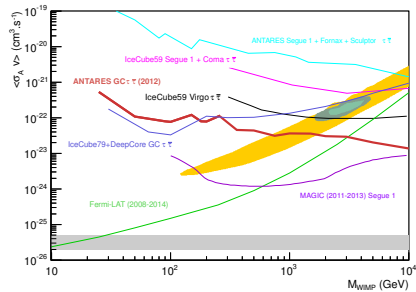


Fig. 17. ANTARES limits on σ_{SD}^p from the Sun as a function of the WIMP mass.

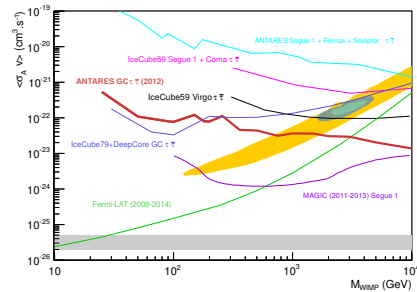


Fig. 18. ANTARES limits on $\sigma_A\nu$ from the Galactic Centre as a function of the WIMP mass.

8. Dark matter and exotics

ANTARES has placed limits on different WIMP dark-matter scenarios by searching for high-energy neutrino emission from WIMP annihilation in the Sun, Earth, Galactic Centre, and dwarf galaxies. Since the dark-matter density is expected to be strongly peaked near the centres of these objects the excellent angular resolution of ANTARES, yields competitive limits for WIMP masses above 50 GeV.

Limits on the spin-dependent (WIMP-proton) interaction cross section σ_{SD}^p from ANTARES observations of the Sun (Fig. 17) [42] and on the WIMP-WIMP velocity-averaged self-annihilation cross section $\sigma_A\nu$ from the Galactic Centre using the $\tau\tau$ channel [41] are given in Fig. 18, and are described in further detail in Ref. [43].

Dark-matter analyses by ANTARES also includes a search for a WIMP signature from the centre of the Earth [44] and a test of secluded dark-matter models in the Sun [45, 46].

ANTARES also places limits on beyond-the-standard-model physics, with searches for magnetic monopoles and nuclearites. Updates to existing limits are presented in Ref. [47].

9. Conclusions

The ANTARES neutrino telescope has proved to be a highly successful instrument, performing a wide range of physics analyses. In particular, its excellent angular resolution on both muon-track and cascade events, facilitated by the excellent optical properties of deep-sea water, is well suited to studying point-like sources of neutrinos. This capability has allowed relevant constraints to be placed upon the the origin of the astrophysical neutrino flux reported by IceCube and in particular any possible galactic contribution. ANTARES will continue data-taking until end of 2016, thus most of the analyses reported here will be extended with an additional three years of data.

References

- [1] M. Ageron, *et al.*, Nuclear Instrum. and Meth. in Physics Research A **656** (2011) 11.
- [2] S. Adrián-Martínez, *et al.*, J. Phys. G **43** (2016) 084001.
- [3] C. Tamburini, *et al.*, PLoS ONE 8(7): e67523. doi:10.1371/journal.pone.0067523.
- [4] J. A. Aguilar, *et al.*, Nuclear Instrum. and Meth. in Physics Research A **626** (2011) 128.
- [5] S. Adrián-Martínez, *et al.*, JINST **7** (2012) T08002.
- [6] S. Adrián-Martínez, *et al.*, ApJ **786** (2014) L5.
- [7] T. Michael, PoS (ICRC2015) 1078.^a; *Light at the End of the Shower: An all-flavour Neutrino Point-Source Search with the ANTARES Neutrino Telescope*, PhD Dissertation, NIKHEF, The Netherlands (2016).
- [8] M. G. Aartsen, *et al.*, Phys. Rev. Lett. **113** (2014) 101101.
- [9] S. Adrián-Martínez, *et al.*, Astrophys. J. **823** (2016) 65.
- [10] M. C. Gonzalez-Garcia, F. Halzen and V. Niro, Astroparticle Physics **57** (2014) 39.
- [11] J. Barrios-Martí, PoS (ICRC2015) 1077.
- [12] M. G. Aartsen, *et al.*, ApJ. **809** (2015) 98.
- [13] T. K. Gaisser, F. Halzen and T. Stanev, Phys. Rep. **258** (1995) 173.
- [14] W. B. Atwood *et al.*, ApJ **697** (2009) 1071.
- [15] F. Krauß, *et al.*, A&A 566 (2014) L7.
- [16] S. Adrián-Martínez, *et al.*, A&A 576 (2015) L8.
- [17] S. Adrián-Martínez, *et al.*, J. Cosmology Astropart. Phys. **12** (2015) 014.
- [18] S. Adrián-Martínez, *et al.*, Astroparticle Physics **36** (2012) 204.
- [19] D. Dornic & A. Sánchez-Losa, PoS (ICRC2015) 1046.
- [20] S. Hümmel, M. Rüger, F. Spanier and W. Winter, ApJ **721** (2010) 630.
- [21] J. Schmid & D. Turpin, PoS (ICRC2015) 1057.
- [22] A. Mathieu, PoS (ICRC2015) 1093.
- [23] E. Waxman and J. Bahcall, Phys. Rev. Lett. **78** (1997) 2292.
- [24] S. Gao, K. Asano, and P. Mészáros, J. Cosmology Astropart. Phys. **11** (2012) 58.
- [25] S. Adrián-Martínez, *et al.*, A&A **559** (2013) A9.
- [26] M. Sanguineti, PoS (ICRC2015) 1068.
- [27] M. Ageron *et al.*, Astroparticle Physics **35** (2012) 530.
- [28] J. Schnabel & S. Hallmann, PoS (ICRC2015) 1065.
- [29] J. A. Aguilar, *et al.*, Physics Letters B **696** (2011) 16.
- [30] M. Honda, T. Kajita, K. Kasahara, S. Midorikawa, and T. Sanuki, Phys. Rev. D **75** (2007) 043006.
- [31] R. Enberg, M. H. Reno, and I. Sarcevic, Phys. Rev. D **78** (2008) 043005.
- [32] S. Hallmann, PoS (ICRC2015) 1059.
- [33] S. Adrián-Martínez *et al.*, European Physical Journal C **74** (2014) 2701.
- [34] C. Lunardini, S. Razzaque, and L. Yang, Phys. Rev. D **92** (2015) 021301.
- [35] M. Su, T. R. Slatyer, and D. P. Finkbeiner, ApJ **724** (2010) 1044.
- [36] A. Neronov, D. Semikoz, and C. Tchernin, Phys. Rev. D **89** (2014) 103002.
- [37] L. Fusco, PoS (ICRC2015) 1055.
- [38] D. Gaggero, D. Grasso, A. Marinelli, A. Urbano, and M. Valli, Ap. J. Letters 815 (2015) L25; PoS (ICRC2015) 489.
- [39] M. Ackermann, *et al.*, ApJ **750** (2012) 3.
- [40] M. Spurio, Phys. Rev. D **90** (2014) 103004.
- [41] S. Adrián-Martínez *et al.*, JCAP **10** (2015) 68.
- [42] S. Adrián-Martínez *et al.*, Phys. Lett. B **759** (2016) 69.

^aPoS (ICRC2015): online at <http://pos.sissa.it/cgi-bin/reader/conf.cgi?confid=236>

- [43] C. Tönnes, PoS (ICRC2015) 1207.
- [44] A. Gleixner & C. Tönnes, PoS (ICRC2015) 1110.
- [45] S. Adrián-Martínez, *et al.*, JCAP **5** (2016) 16.
- [46] M. Ardid & C. Tönnes, PoS (ICRC2015) 1212.
- [47] I. El Bojaddaini & G. E. Pávālas, PoS (ICRC2015) 1060.